



Experimental Study of the Principal Characteristics of Sustainable Micropile Grout Containing Alternative Sands

Dao Phuc Lam ¹, Nguyen Van Manh ^{2,3} , Pham Thi Nhan ^{2,3}, Le Huy Viet ^{2,3} ,
Tang Van Lam ^{2,3} , Dang Van Phi ^{2,3}, Ngo Xuan Hung ^{2,3} , Piotr Osinski ^{3,4} ,
Kennedy C. Onyelowe ^{3,5} , Bui Van Duc ^{2,3*} 

¹ Faculty of Civil Engineering, University of Transport Technology, Hanoi, Vietnam.

² Faculty of Civil Engineering, Hanoi University of Mining and Geology, Hanoi, Vietnam.

³ Geotechnical Engineering, Construction Materials and Sustainability Research Group, Hanoi University of Mining and Geology, Hanoi, Vietnam.

⁴ Institute of Civil Engineering, Warsaw University of Life Sciences, 02-787 Warsaw, Poland.

⁵ Department of Civil Engineering, Michael Okpara University of Agriculture, Umudike, Nigeria.

Received 08 June 2024; Revised 21 September 2024; Accepted 28 September 2024; Published 01 October 2024

Abstract

The paper discloses a laboratory investigation on employing manufactured sand cement as grout in micropiling works. In practice, to prepare micropile grouts, Portland cement is commonly used. The grout usually consists of natural sand to obtain the strength parameters and value international standards require for micropile construction. It is common knowledge that using concrete and natural sand leaves its environmental footprint. Although there have been numerous attempts to use more environmentally friendly materials, utilizing manufactured sands, particularly for micropile grouting, is a scientific challenge that researchers are still trying to address. The present study investigates the performance of micropile grout mixtures containing manufactured (M) sands, including limestone (L-M) and granite (G-M) rock as replacements for natural sand. For this purpose, laboratory tests, including unconfined compression strength (UCS) and workability tests, were conducted on samples with varying compositions and ratios of L-M and G-M materials. The complementary microstructure and chemical composition analyses were performed using scanning electron microscopy (SEM) and energy-dispersive X-ray spectroscopy (EDS) analysis. The laboratory results indicate that the UCS at 28 days of hardening for all M-sand cement mixtures exceeds the minimum standards required values, falling in a range of 40-50.2 MPa. It's noteworthy that the strength of cement grout containing L-M sand was found to be higher than that of G-M sand. The SEM results show the G-M sand grain is rougher than L-M, and the L-M sand grain size is finer than the G-M samples, which causes a decrease in porosity at the interfacial transition zone. Grout workability tests demonstrated that higher water-cement ratios (W/C) led to increased fluidity across all mixtures, with G-M sand resulting in lower flowability than L-M samples. Overall, the results suggest that the proposed mixtures could serve as sustainable alternatives for micropiling, reducing cement content and utilizing alternative, reused materials in grouting mixtures more effectively and sustainably.

Keywords: Alternative Sands; Crushed Stones; Micropile; Grout Strength; Microstructure of Grout.

1. Introduction

Nowadays, geotechnical engineering provides multiple methods of improving ground conditions to meet the requirements for safe infrastructure design. Ground improvement technologies assist the design in foundation engineering, as well as slope stability issues and other design challenges when complex soil-structure interactions are

* Corresponding author: buivanduc@humg.edu.vn

 <http://dx.doi.org/10.28991/CEJ-2024-010-10-019>



© 2024 by the authors. Licensee C.E.J, Tehran, Iran. This article is an open access article distributed under the terms and conditions of the Creative Commons Attribution (CC-BY) license (<http://creativecommons.org/licenses/by/4.0/>).

considered. Ground reinforcements are aimed at improving the bearing capacity of the areas with poor geotechnical conditions. The reinforcing effect is governed by the shear, tensile strength, and the bonding effect that the supporting structure develops within the subsoil. During the analysis and design phase, while choosing the reinforcing method, considerations such as bearing capacity, structural integrity, and stability control are crucial for ensuring safety. This would allow for minimizing settlements and enhancing the overall durability of structures. These factors are essential for meeting serviceability requirements, addressing construction challenges, and optimizing economic factors [1]. One of the methods of ground improvement that has been successfully applied in geotechnical engineering for over 60 years is micropiling [2]. Micropiles with a nominal diameter of less than 300 mm have been widely employed in numerous applications, including structural support for foundations, static and seismic retrofitting, minimizing uplift forces impact, and slope stability improvement. The micropiling technology was initially developed in Italy in 1952 [2, 3]. The method is now commonly used due to its engineering benefits, such as efficient installation in space-constrained conditions, high grout-ground bond strength, low impact on nearby structures, and installation on elevated groundwater table conditions [4-6].

Among the structural components of micropiles, grout is considered one of the key elements that increase a micropile's load-bearing capacity as well as the load transfer behavior [7]. Thus, applied grout properties must meet specific requirements of grout consistency or flowability and strength [8]. Although the unconfined compressive strength (UCS) mostly depends on the design purposes, a 28-day strength requirement for micropiles between 28 and 35 MPa is widely accepted [5]. In general, grouts used for micropiles constitute a mixture of cement and water; in specific cases, additives such as retarders, plasticizers, and binding agents enhance the grout properties [5]. The main component of the grout for the micropile structure is cement. According to ongoing global debate, the use of cement is considered to be a significant environmental threat due to its greenhouse gas footprint. Cement production is considered harmful to the environment mainly due to the synthesis of CaO in the chemical reaction resulting in carbon dioxide (CO₂) emission and water vapor released at high temperatures [9]. CO₂ is widely recognized as one of the major greenhouse gases that contributes significantly to the global warming effect [10, 11], accounting for 65% of all greenhouse gases emitted to the atmosphere [12]. Additionally, using excessive amounts of cement in grouting could increase the overall cost of micropiling work. Hence, adding filling materials in place of cement while upholding the same grout properties as per design requirements can be a reasonable approach to achieve both economic and environmental benefits. To date, many efforts have been continuously put into reducing the amount of cement used in the construction industry in general and in grouting works in particular. That is why, using silica gels (known as organic grouts) and sand dredging from river beds, or organic grouts, have been outlawed due to reports proving the contamination risk of groundwater [13]. The most recent research studies show bio-grout efficiency, although the durability has not yet been examined [14]. Similarly, many negative impacts, including physical, biological, and anthropogenic environmental impacts of river sand mining, were presented by Rentier & Cammeraat (2022) [15]. Notably, mining river sand affects areas far beyond the actual exploration site boundaries. Several researchers have investigated the feasibility of utilizing industrial wastes and industrial by-products, such as fine quartz powder, coal bottom ash, crushed rocks, steel slag, oil-contaminated drilling waste, etc., in grout as a replacement for river sand and even cement [7, 16-22]. In the application of micropiling works, fly ash is one of the most popular active additions since it could enhance the properties of cement-based materials due to the pozzolanic reactions leading to new hydrated phases [23]. This approach, utilizing industrial by-products, may lessen the amount of land needed to dispose of industrial wastes. Among those alternative construction materials, manufactured sand (M-sand), produced by processing the by-products of rock quarries, is one of the practical substitutes for cement in both grout and concrete mix in many regions in the world, especially in Vietnam since it is widely available due to three-quarters of Vietnam being a mountainous region.

According to earlier studies, the strength parameters of concrete made using M-sand meet the values of commonly used concrete mixtures. This means that M-sand can be utilized as a reasonably priced and easily accessible substitute for river sand, leading to fewer negative impacts on the environment due to the low excessive mining of river sand [24, 25]. According to the review given by Arulmoly & Konthesingha (2022) [26], examining alternatives to river sand in concrete, the manufactured sand could be considered useful due to its angularity, rough surface, higher total specific surface, and lower presence of harmful substances compared to river sand. These characteristics influence the performance of cement-based mixes, with studies showing both positive and negative outcomes. When it comes to using granite crushed particles, that is a matter of investigation of the present paper; the work performed by Joel (2010) [27] revealed that at 28 days, the peak compressive strength of granite fine cement mixtures was improved by as much as 20% when comparing to tested samples made of river sand. The research results presented in Li et al. (2016) [28] proved that introducing granite dust reduces the early strength of concrete. However, when the replacement ratio is kept within 20%, the manufactured sand concrete exhibits higher long-term compressive strengths, bending strengths, and elastic moduli. Experimental and numerical analysis performed by Bacarji et al. (2013) [29] demonstrated a strong correlation between concrete compressive strength and the cement-granite replacement ratio. The research results confirmed that granite could be a sustainable cement replacement. More studies on crushed stone replacements in concrete revealed that manufactured sand containing up to 13% stone powder enhances the long-term tensile strength of MSC. There is a rapid increase in the first 28 days, which then slows. Optimal stone powder content (up to 13%) boosts tensile strength

when the water-cement ratio is ≥ 0.45 ; for ratios < 0.45 , up to 9% stone powder is beneficial [30]. The literature review clearly shows that most of the published research focusing on using alternative resources in concrete mixtures has not been performed for more specific engineering purposes, such as a grout mixture applied in ground improvement methods. Furthermore, it is not common practice to consider using alternative cement grouts for micropiles that contain M-sands.

The construction industry's ongoing efforts to reduce cement usage have led to the exploration of alternative materials for grouting. Traditional practices, such as silica gels and riverbed sand, have been banned due to environmental concerns, particularly the risk of groundwater contamination. The impact of river sand mining extends beyond extraction sites, prompting researchers to investigate the viability of industrial wastes and by-products as substitutes for both river sand and cement in grouting applications. Recent studies proved that using by-products such as crushed stones (granite or limestone) from open-pit mines could be an effective alternative to commonly used cement mixtures [24–30]. However, none of them fully investigated the impact of grain size on the shear strength of the mixtures nor the workability or microstructure influencing the general performance of the grout used in micropiling works. Bearing all that in mind, the scientific gap that the present paper aims to fill is to evaluate the potential use of grouts prepared with two types of M-sands made of limestone and granite rock. To evaluate such grout performance, three crucial characteristics of grout mixtures, including strength properties, workability, and microstructure, were examined and discussed throughout the paper.

2. Materials and Testing Program

2.1. Laboratory Samples' Characteristics

The samples used for M-sand cement grout mixtures consist of Portland Cement Blended 40 (PCB-40), modified sand particles including crushed limestone (L-M) and granite rock (G-M), and water. The specific surface and specific gravity of PCB-40 were $3600 \text{ cm}^2/\text{g}$ and 3.15, respectively. The L-M and G-M sand samples were obtained from stone quarries in Ha Nam and Ninh Thuan Province, Vietnam. The collected portions of crushed M-sand were sieved to obtain maximum grain sizes of 5.0 mm as suggested in the Vietnam national standard, TCVN 9205:2012 [31]. Table 1 presents the physical properties of two M-sand types (L-M and G-M). Figure 1 shows the M-sand samples prepared for laboratory analyses.

Table 1. Physical properties of M-sands

| Description | Units | Type of M-Sand | |
|------------------|------------------------|----------------|--------------|
| | | Limestone | Granite rock |
| Specific Gravity | - | 2.661 | 2.665 |
| Bulk Density | kg/m^3 | 1.406 | 1.419 |
| Moisture Content | % | 13.3 | 13.1 |
| Porosity | % | 47.2 | 46.7 |
| Fineness Modulus | - | 3.36 | 3.38 |



Figure 1. Manufactured sands used in this investigation

L-M and G-M grain sizes were determined using the dry sieve analysis according to the ASTM D422 standard testing method. According to the results of the sieving test, the M-sand samples used in the study were classified as well-graded materials of grain sizes. Additionally, the grain size of particles of G-M sands is larger than that of L-M. These grain

characteristics, including the uniformity and larger grain size of L-M, could potentially affect the density of the interfacial transition zone (ITZ) due to the wall effect proposed by Ollivier et al. (1995) [32], subsequently the strength development of L-M cement grout. The grain size distribution curves of the M-sands are shown in Figure 2. Two additives, including acrylic-based plasticizer and acrylic polymer plasticizer, were added to the mixtures to enhance the workability of M-sand cement grouts. The former was used to improve workability with its primary functions being to disperse cement grains and facilitate a gradual onset of cement hydration. The latter was to achieve greater mechanical strength at an early age.

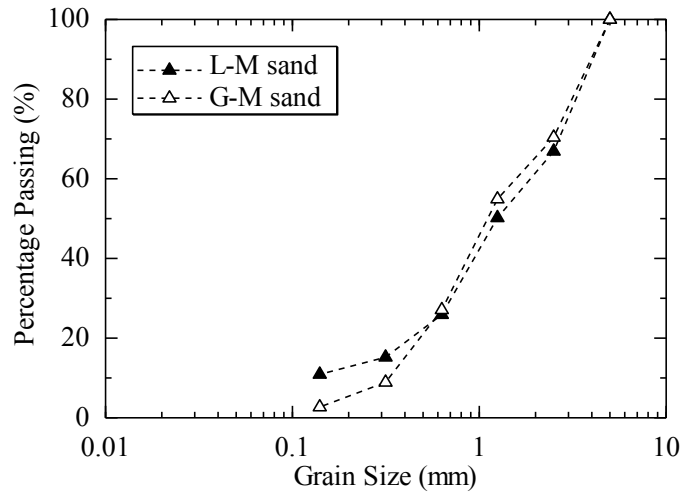


Figure 2. Particle size distribution curves of L-M sand and G-M sand

Figure 3 shows the diagram illustrating the experimental process. The manufactured sand samples were initially sieved; all particle sizes with diameters less than 5.0 mm were employed in the subsequent experimental procedures, which involved the strength development and microstructural characteristics of manufactured sand cement grouts and the particle size analyses.

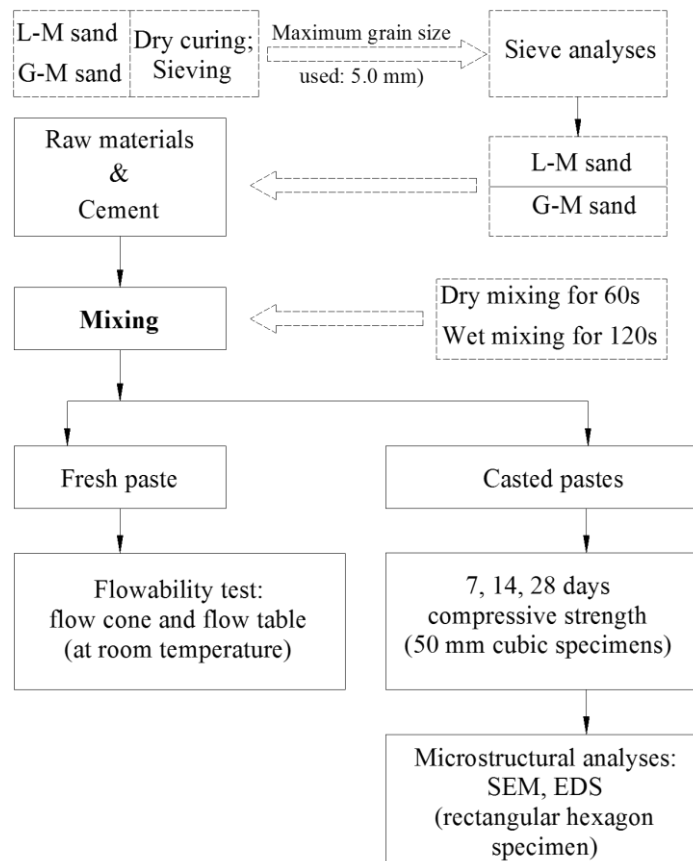


Figure 3. Experimental flow chart

2.2. Grout mixture Composition and Ratios

All grout mixtures used in the study were prepared in compliance with ASTM C305. The method of absolute volume was employed to propose the mixture ratios. A total of twenty-seven grout specimens were prepared. The cubic samples (50x50 mm) compositions are listed in Table 2, where water/cement (W/C) ratios fell in the range of (0.4 - 0.5) for type A micropiles (gravity fill by weight technique) as suggested by FHWA (2005) [5] and Bruce & Juran (1997) [33].

Table 2. Mixture compositions used in the study

| Mix No. | W/C | Materials | | M-sands (kg) | | Additives (% by weight of cement) | | Number of cubic specimens |
|---------|------|-------------|-----------|--------------|---------|-----------------------------------|-----------------|---------------------------|
| | | Cement (kg) | Water (l) | Limestone | Granite | Acrylic based | Acrylic polymer | |
| M1 | 0.43 | 593 | 255 | 1441 | 1444 | 1.5 | 1.0 | 9 |
| M2 | 0.45 | 567 | 255 | 1466 | 1468 | 1.5 | 1.0 | 9 |
| M3 | 0.50 | 510 | 255 | 1517 | 1520 | 1.5 | 1.0 | 9 |

2.3. Compressive Strength Test

The strength of M-sand cement grout specimens was investigated by performing an unconfined compression test following the ASTM C109/AASHTO T106 standard test procedure [5]. Three cubic specimens from each of the three grout mixtures (M1, M2, and M3) were tested at three different curing times to obtain the representative strength results, i.e., 7, 14, and 28 days. The average strength values were recorded using the automatic controller. The strength tests were performed using a universal test machine with a capacity of 500 kN. During the test, the specimen was gradually subjected to a compressive load at a constant rate of 0.5 MPa/s until the specimen failed. The measured compressive strength of the cube samples was calculated using the recorded maximum applied load and divided by the specimen area. Figure 4 shows the sample preparation for the strength test. The samples were prepared in a mold for proposed ratios and composition of constant water content and mixed proportions of limestone and granite materials. After 2 days of casting, the M-sand cement grout specimens were removed from the mold and then immersed in all the study specimens until the strength test was conducted.



Figure 4. Preparation of M-sand cement grout samples for compressive strength test

2.4. Workability Test

The pumpability of grout is an essential requirement in the production of micropiles [5]. The fluidity and flowability of M-sand cement grouts were thoroughly examined using both flow cone and flow table tests at room temperature ($23\pm 2^{\circ}\text{C}$) according to ASTM C230/C230M-20 [34] and ASTM C939-10 [35]. Three different proportions of water to cement, 0.43, 0.45, and 0.5, were used for testing. Initially, the flow cone test determining fluidity was conducted for all the M-sand cement grout mixtures. The flow cone characteristics were a height of 190 mm, a capacity of 1725 ± 5 mL, and an internal orifice diameter of 12.7 mm. Grout was filled up to reach the calibration height, and then the duration of the grout pouring was recorded to determine flow time. The spread flow test was then conducted following ASTM C939-02. The principle of the spread flow test is to fill a cylinder with a specified volume of grout (250 ml) and then pour the mixture onto a scaled plate from a height of 1 cm. The flowability of the grout was determined by measuring the diameter of the grout covering the measuring plate, as shown in Figure 5.



Figure 5. M-sand cement grout flowability measurement using spread flow test

2.5. Microstructure Analyses

A QUANTA system with scanning electron microscopy (SEM) and energy-dispersive X-ray spectroscopy (EDS) analysis was used to establish the microstructure characteristics of the M-sand cement grout mixtures. The QUANTA system setup is presented in figure 6. The SEM and EDS tests were performed at the Hanoi University of Mining and Geology, Vietnam laboratory. SEM technology is based on the collision effect of accelerated high-energy particles present on the surface of the sampling material. The interaction between the material surface and the emitted beam allows precise imaging of material surface topography, chemical properties, crystalline nature, and homogeneity. Energy dispersive X-ray spectroscopy is an analytical technique used for the elemental analysis and chemical characterization of a sample. Characteristic X-rays of a specimen are stimulated by the incident electron beam in an SEM. Combining the SEM and EDS helps establish alkali-aggregate interactions in concrete samples, allowing the identification of any potential structure faults.



Figure 6. Laboratory setup of QUANTA system

Figure 7 illustrates the sample prepared for SEM and EDS analysis. The samples were stored in dry conditions for 28 days after curing and then were trimmed into a rectangular hexagon specimen of 25×40 mm² in dimension. The grinding and polishing procedures were conducted on sample surfaces to ensure the appropriate roughness of samples for SEM and EDS tests.

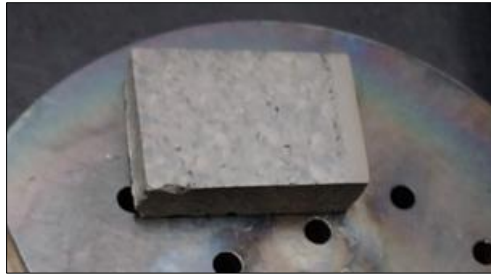


Figure 7. Sample prepared for SEM and EDS analysis

3. Results and Discussion

3.1. Unconfined Compressive Strength Results

The required strength of cement grout for micropiles depends on each specific case; however, in available international standards, including AASHTO and European codes, the minimum strength ranges from 28 to 35 MPa according to FHWA (2005) [5] and 25 MPa according to the EN 14199 European standard [36]. The results of the UCS of M-sand cement grouts are shown in Figures 8-a and 8-b. The laboratory results show that the samples prepared with higher W/C ratios have experienced lower strength, a common effect for such prepared samples. The compressive strength increases with curing time, regardless of the W/C ratio and type of M-sand used (L-M or G-M).

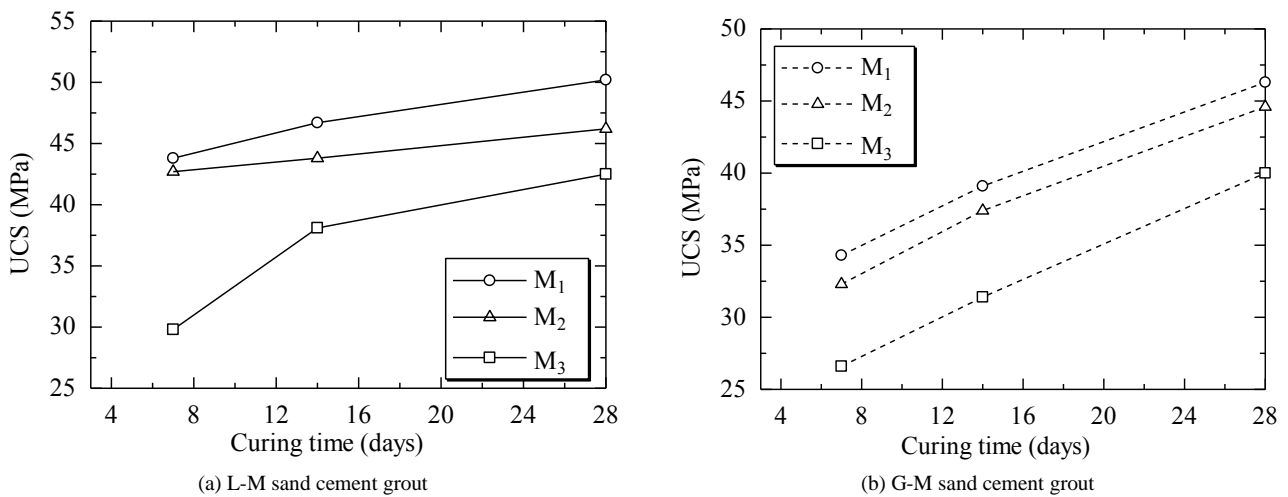


Figure 8. Compressive strength of M-sand cement grouts

Considering strength requirements, it can be noted that both M-sands mixtures, including limestone and granite rock, present applicational potential in micropiling works. Figure 9 presents the UCS laboratory test results for 28 days of curing time, with references to international standard values required for grout strength, determining the application in soil reinforcement works.

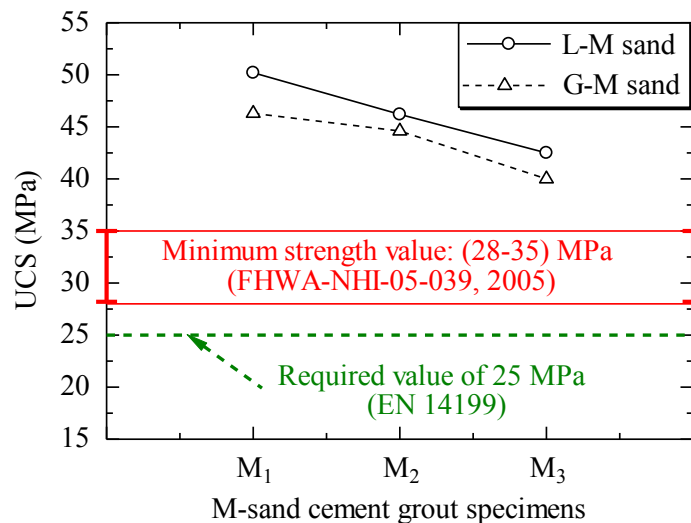


Figure 9. 28-day compressive strength of M-sand cement grouts

Worth noting is that the UCS at 28 days of hardening of L-M samples was greater than that of G-M, in which the grout mixture M1 yields the highest value of UCS, 50.2 MPa. Such behavior could be attributed to the grain size characteristics of the L-M sand used in the study. In particular, the grain size distribution of L-M sand is more uniform, and the particle diameter of L-M is less than that of G-M. These two features, including uniformity and finer grain, cause a higher packing density of the L-M sand cement grout, which is in agreement with available research results reporting that using finer sand grains in the grout matrix could contribute to the higher compressive strength [37–40]. Earlier studies revealed that using limestone sand could cause the chemical reaction between calcite and cement paste, leading to a superficial etching of aggregates (i.e., sand particles), and due to the etching effect, the bond strength was enhanced [41]. The bond strength between particles and cement paste using limestone/granite was also investigated by Ollivier et al. (1995) [32] and Zimbelmann (1987) [42]. They found that the use of limestone resulted in a larger bond strength compared to that of granite, as shown in figure 10. Moreover, according to Jambor (1986) [43], the hydrate reaction leads to an improvement in the compactness of the paste, resulting in an improvement of the physical properties of the ITZ around the calcareous particles [32, 43].

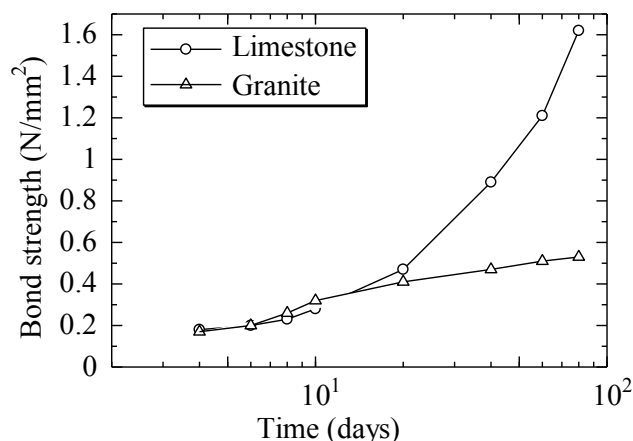


Figure 10. Development of adhesion between particles and cement paste using limestone/granite (modified after [32, 42])

3.2. Workability Test Results

3.2.1. Flow Cone Test

The flow time results for all study scenarios are shown in Table 3. The flow time of all analyzed mixtures increases as the W/C increases, in which the efflux time of G-M sand cement grout is larger than that of L-M samples. However, all M-sand grouts exceeded the limit value of efflux time at 35s. Consequently, the flow table method was then chosen as an alternative test for determining the workability of the cement grout recommended in ASTM C939-02. The flow cone test results clearly show that for samples where M-sand was not present, the required value (35s) for none of the mixtures (M1, 2 and 3) was not met. The efflux time in all the mixtures was lower for the limestone samples, which could be associated with the chemical characteristics of the additive, which is less stable than the granite crushed stone.

Table 3. Flow time test results

| Grout Mix No. | Efflux time in ASTM C939 cone (sec) | | Required value (sec) | Without M-sands in cement grout (sec) |
|---------------|-------------------------------------|---------|----------------------|---------------------------------------|
| | Limestone | Granite | | |
| M1 | 93 | 105 | | 32 |
| M2 | 78 | 91 | Max: 35 | 24 |
| M3 | 70 | 82 | | 18 |

3.2.2. Spread Flow Table Test

Laboratory test results on the spread flow properties of M-sand cement grouts using the flow table method are shown in Figure 11. The results indicate the higher W/C ratio yields a higher fluidity value for all study mixtures. Using G-M sands in cement grout could lead to lower flowability compared to that of L-M. It is observed that at the W/C ratio of 0.5, the fluidity of L-M and G-M are 25.1 cm and 24.7 cm, respectively. The reason for these behaviors could be explained by the difference in the roughness of manufactured sands used in this study. As reported by Arulmoly & Konthesingha (2022) [26], granite dust could influence the performance of the mixture; thus, the workability decreases could be associated with increased chloride penetration while using granite particles in the grout mixture.

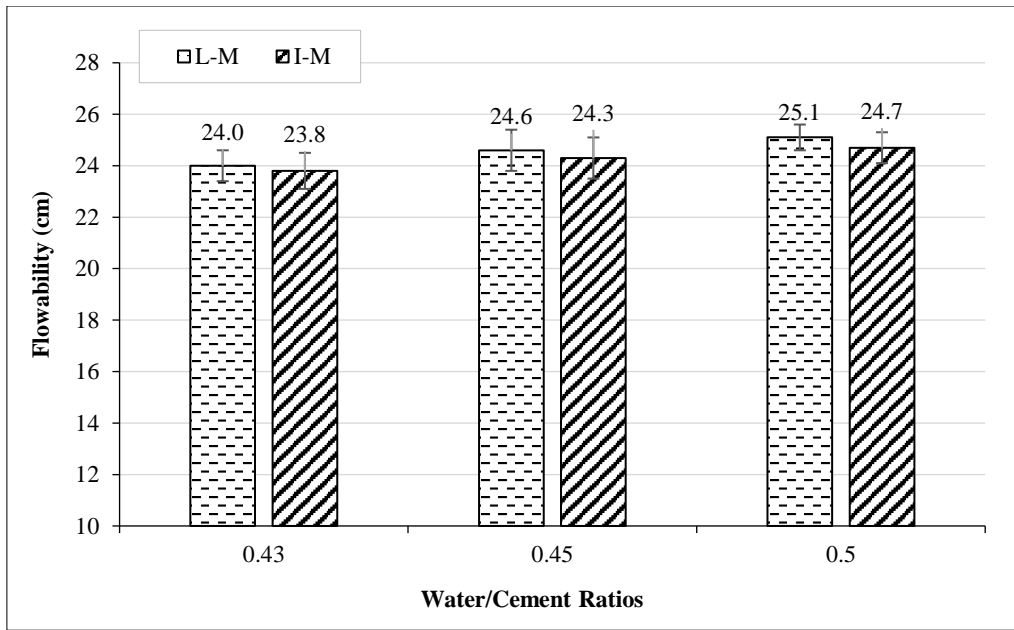
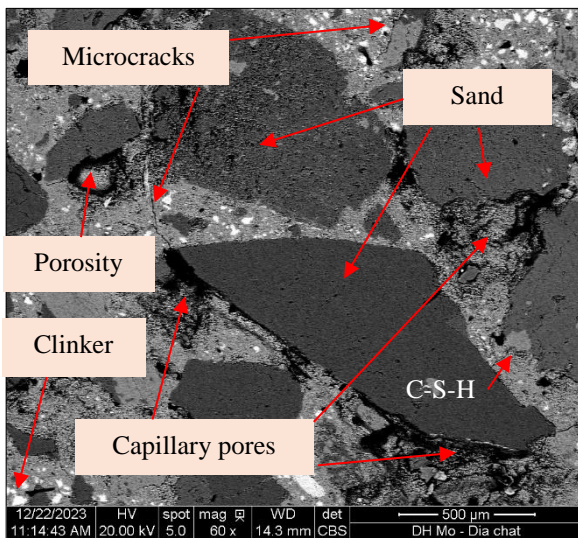


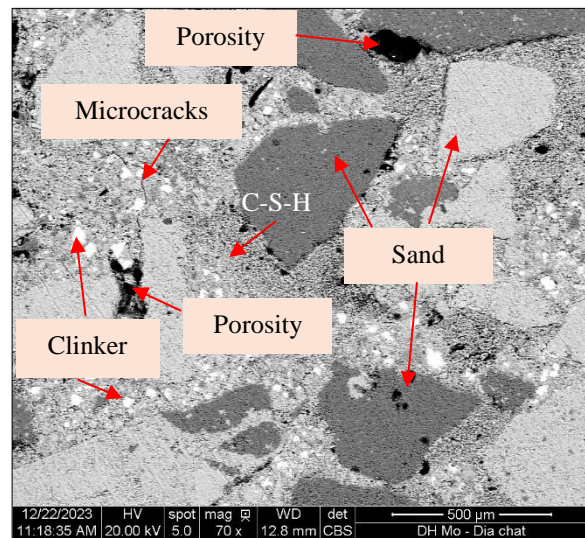
Figure 11. Flow table test results of M-sand cement grouts

3.3. Microstructural Analyses

Figures 12 to 14 present the SEM test results of cement grouts made with G-M and L-M sands at different magnifications from 500 μm to 100 μm. The different microstructures, including C-S-H, clinker, porous areas, microcracks, and sand, were also observed, as shown in figure 12. It can be seen that the particle sizes of G-M sand are greater than those of L-M sand. This finding is consistent with the results of particle composition analysis as illustrated in figure 2. In addition, matrices using G-M sand exhibited higher porous areas, such as porosity and capillary pores, than the matrices containing L-M sand. This indicates that smaller sand produces a higher matrix quality, which is more homogeneous, denser, and has a lower number of microcracks. Matrices with G-M sand exhibit more microcracks compared to those using L-M sand. This is due to the presence of numerous porous areas in G-M’s matrices, particularly capillary pores, which have lower strength and make it easier for microcracks to form and propagate (Figure 12). The findings in Akçaoğlu et al. (2004) [44] indicated that the matrix using larger aggregates combined with a low water-to-cement ratio led to more critical ITZ with more microcracks. Furthermore, Lyu et al. (2020) [45] and Elsharief et al. (2003) [46] observed that decreasing the size of aggregates generally leads to a reduction in matrix porosity. The investigation of Scrivener et al. (2004) [47] also confirmed that the use of larger and rougher aggregates led to a thicker ITZ with more microcracks.



(a) G-M sand cement grout



(b) L-M sand cement grout

Figure 12. SEM images of matrices using G-M and L-M sand

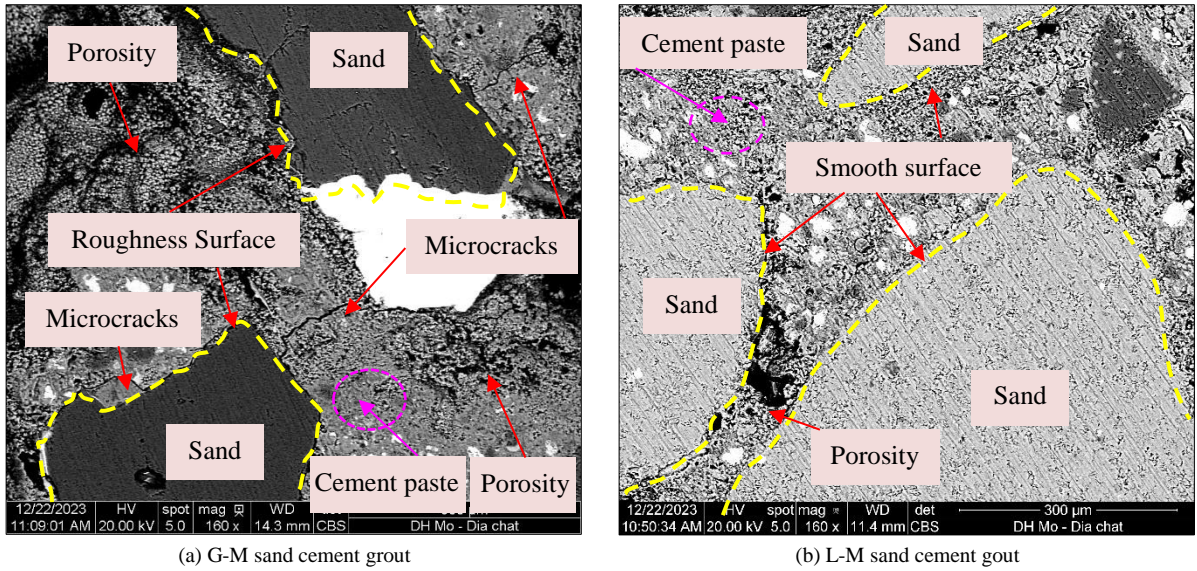


Figure 13. SEM micrographs of M-sand surfaces

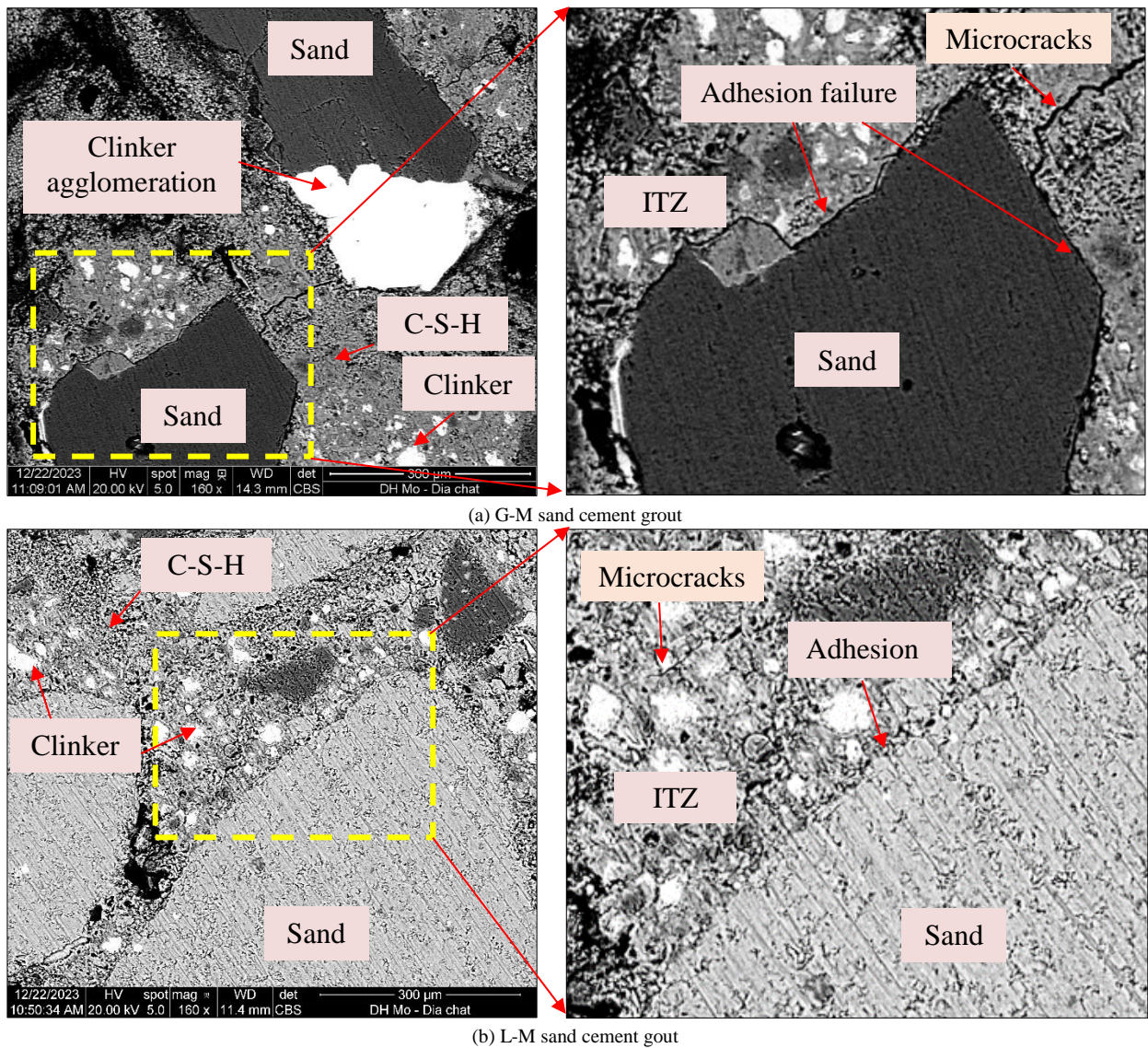


Figure 14. SEM micrographs of matrix transition zone: (a) G-M cement grout, and (b) L-M cement grout

In addition, observing the surface texture of M-sand particles on SEM images at the magnification of 300 μm, it was found that the surface texture of G-M sand particles was rougher than that of L-M sand, as shown in Figure 13. Moreover,

cement grout containing G-M sand was porous with recorded microcracks, whereas cement grout containing L-M sand was more homogeneous and denser. This behavior could be attributed to the size of L-M sand being finer than G-M sand samples. The matrices using finer sand grains produced higher local stiffness with reduced porosity at the ITZ surrounding aggregates as well as the fiber and matrix [38-40, 48].

Figure 14 shows the SEM image of microstructures at the ITZ surrounding matrix and aggregates corresponding to G-M and L-M sand cement grout specimens. The G-M sand cement grout experienced bond failure at the interface matrix and sand with adhesion failure, as shown in figure 14a. This could be explained by the fact that G-M sand contained a larger grain size than L-M sand, leading to the matrix containing G-M sand producing lower packing density than the matrix incorporating L-M sand [48]. However, the adhesive failure behavior at the ITZ was not observed in the case of L-M cement grout. This could be attributed to the reactivity of limestone sand with Portland cement paste [41] and the superficial etching effect on limestone sand particles [49]. Farran (1957) [41] and Grandet & Ollivier (1980) [49] reported that the chemical reaction between calcareous sand and Portland cement paste took place. This led to the formation of the calcium aluminate hydrate, due to the paste hydration during the reaction of the calcium carboaluminate ($C_3A.CaCO_3.11H_2O$). The process was followed by the reduction in the porosity of L-M's ITZ and an increase in the compactness of the paste, resulting in the superficial etching of limestone particles. Consequently, the entire process led to an improvement of the microstructure of the ITZ around the limestone particles, as observed in figure 14b, where no adhesive crack could be noticed.

SEM Figures 12 to 14 indicate both G-M and L-M sand cement grouts exhibit a higher porosity at ITZ compared to the cement paste. This behavior of M-sand cement grouts could make them more susceptible to microcracking-induced self-desiccation due to their weak structure; these findings are in accordance with Gaboczi (1990) [50] and Monteiro (2006) [51]. Wong and Buenfeld (2009) [52] proved that the chemical composition of aggregates can affect the reaction between the aggregate and the cement paste as well as the characteristics of ITZ. The chemical composition of calcium silicate hydrate (C-S-H) phases at ITZ was determined by using EDS analysis, as shown in Figure 15.

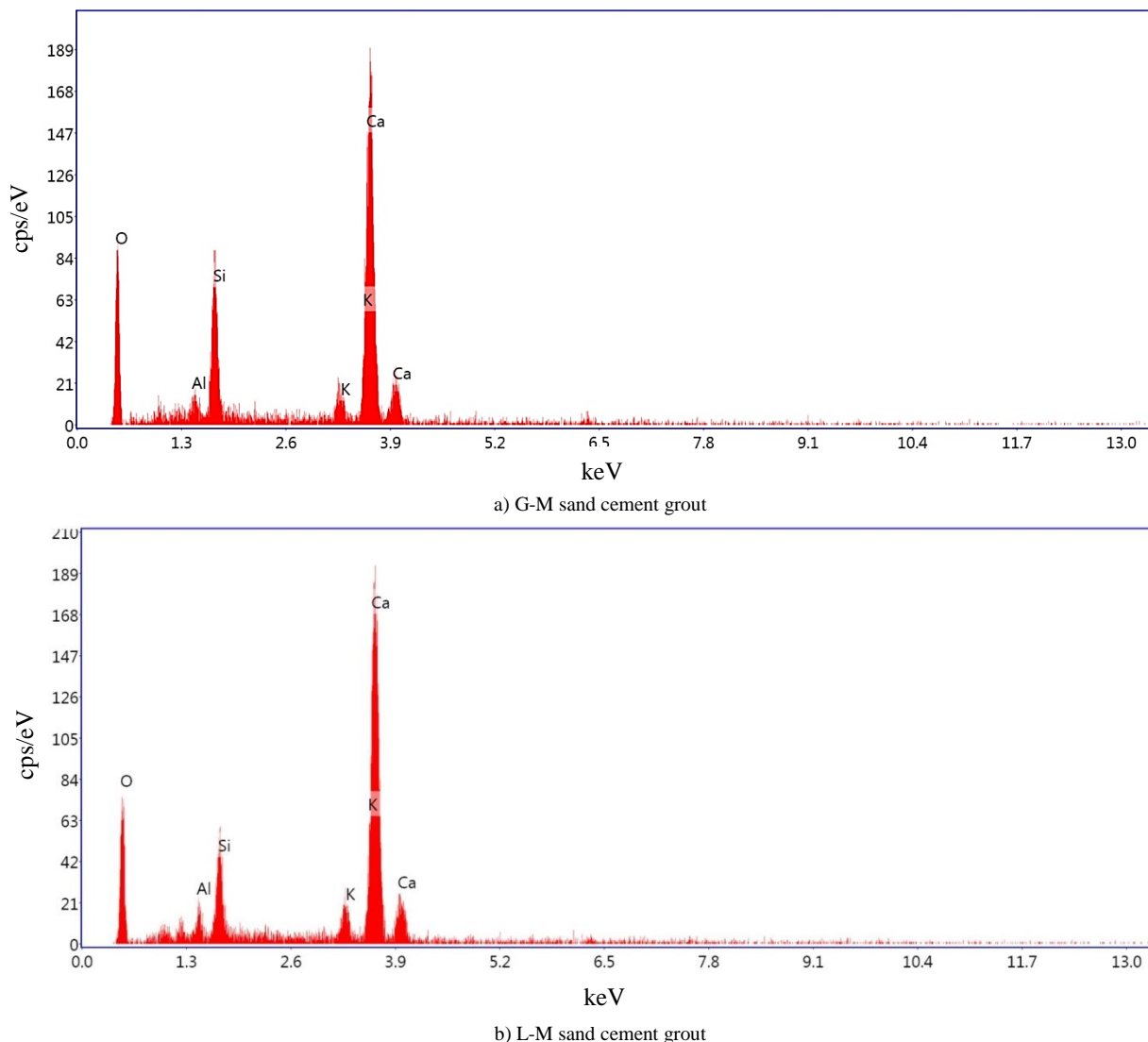


Figure 15. Typical results of the C-S-H phase of M-sand cement grouts using the EDS method

From Figure 15, it can be inferred that Calcium (Ca), Silicon (Si), and Oxygen (O) are the main components of the M-sand cement grout specimens. The G-M samples presented higher Si content than L-M sand cement grout. Table 4 shows the atomic elements measured in the vicinity of aggregate (crushed sand particle); the recorded Ca/Si ratios of G-M and L-M were 3.07 and 5.13, respectively.

Table 4. Atomic densities of C-S-H phases based on EDS analyses

| Descriptions | Elements | | | Ca/Si ratios |
|---------------------------|----------|------|-------|--------------|
| | Ca | Si | O | |
| Atomic elements (%) (G-M) | 19.39 | 6.32 | 71.78 | 3.07 |
| Atomic elements (%) (L-M) | 21.51 | 4.19 | 71.74 | 5.13 |

According to Yuan & Odler (1987) [53], the magnitude of Ca/Si of 3.07 in the L-M grout indicates that the C-S-H phase is formed and located on the outermost boundary of the ITZ, at the distance of 120 μm from the sand grains surface. However, in the case of L-M grout, the value of Ca/Si was 5.13, implying that C-S-H phase was right next to the grain surface leading to a denser of ITZ since the voids in the ITZ were filled with the C-S-H, Carboaluminates, and anhydrous silicates. Subsequently, increased compaction of ITZ was gained. This aligns with the findings of Ollivier et al. (1995) [32], which indicated that the chemical reactions at the interface between the aggregate and the cement paste can either weaken or strengthen the ITZ, depending on the compatibility of the materials.

4. Conclusion

The present research evaluates the application potential of the grout mixture used for microfilming. It investigates the performance of the mixtures containing limestone and granite rock material as a replacement material for natural sand. For that purpose, the laboratory tests, including unconfined compression strength and grout flow tests, were performed for samples of different compositions and ratios of L-M and G-M material. The laboratory tests revealed that the UCS at 28 days of curing time for L-M sand cement grout was greater than that of G-M, and the strength of all studied M-sand grout mixtures is higher than the minimum required value for micropiling works. The consistency test revealed that the use of M-sands in cement grout could result in a higher efflux time since all the flow cone measurement results of the three study mixtures didn't meet the suggested value of 35s. Using the spread flow test, it was found that the larger W/C ratio yielded a higher fluidity value for all analyzed mixtures. The test results proved that using G-M sands in cement grout could lead to lower flowability when compared to L-M samples. The microstructure of M-sand cement grouts, including SEM and EDS. The SEM analyses showed the differences in the roughness on the boundary surfaces of L-M and G-M samples. The images captured for grout containing G-M sand revealed the presence of microcracks, whereas cement grout containing L-M sand was more homogeneous and denser. According to the EDS analyses, results revealed the occurrence of bond failure and cracking at the interface matrix of the grout containing G-M sand. Such observation raises the concern of potential use in refinement applications. However, the scale of the effect is found to be similar to the conventional material used in micropiling. When it comes to the analyses of the atomic density of C-S-H phases, the cement grouts containing G-M or L-M sand did not show significant differences, meaning that the use of M-sands does not contribute to the hydration process in cement grout. The set of performed tests and, more importantly, the obtained results allow concluding that the proposed mixtures could successfully serve as an alternative material for micropiling works, especially in terms of grout strength requirement. However, when considering using crushed rock grout mixtures for micropiling works, particular attention must be paid to the grout pumping technique. Due to the low grout fluidity examined in the laboratory (less than 35s), the effectiveness and stability of the micropiling works could be affected.

5. Declarations

5.1. Author Contributions

Conceptualization, D.Ph.L., N.V.M., and B.V.D.; methodology, D.Ph.L., N.V.M., and B.V.D.; validation, Ph.T.Nh., L.H.V., T.V.L., N.X.H., P.O., and K.O.; formal analysis, B.V.D., N.V.M., D.V.Ph., D.Ph.L., and P.O.; investigation, N.V.M., B.V.D., P.O., and D.Ph.L.; resources, N.V.M., B.V.D., and D.Ph.L.; data curation, N.V.M., B.V.D., and D.V.Ph.; writing—original draft preparation, B.V.D., N.V.M., D.Ph.L., D.V.Ph., and P.O.; writing—review and editing, B.V.D., N.V.M., D.Ph.L., D.V.Ph., and P.O.; visualization, L.H.V., T.V.L., N.X.H., Ph.T.Nh., and K.O.; supervision, N.V.M. and B.V.D.; project administration, N.V.M.; funding acquisition, N.V.M. All authors have read and agreed to the published version of the manuscript.

5.2. Data Availability Statement

The data presented in this study are available on request from the corresponding author.

5.3. Funding

This research was supported by the Vietnam Ministry of Education and Training through the project code: B2023-MDA-07.

5.4. Acknowledgements

The authors gratefully acknowledge financial support from the Vietnam Ministry of Education and Training through the project code: B2023-MDA-07. The authors would like to acknowledge the support from Hanoi University of Mining and Geology, Hanoi, Vietnam.

5.5. Conflicts of Interest

The authors declare no conflict of interest.

6. References

- [1] Eslami, A., Moshfeghi, S., MolaAbasi, H., & Eslami, M. M. (2020). Background to foundation engineering. Piezocone and Cone Penetration Test (CPTu and CPT) Applications in Foundation Engineering, Elsevier, Amsterdam, Netherlands. doi:10.1016/b978-0-08-102766-0.00002-x.
- [2] Thomas F. H. (2007). 4th Lizzi Lecture: Historical Review and Analysis of 55 Years of Micropiles. Proceeding 8th IWM, 26-30 September, 2007, Toronto, Canada.
- [3] Bruce, D. A., DiMillio, A. F., & Juran, I. (1997). Micropiles: the state of practice Part 1: Characteristics, definitions and classifications. Proceedings of the Institution of Civil Engineers - Ground Improvement, 1(1), 25–35. doi:10.1680/gi.1997.010104.
- [4] Elsaied, A. E. (2014). Performance of footing with single side micro-piles adjacent to slopes. Alexandria Engineering Journal, 53(4), 903–910. doi:10.1016/j.aej.2014.07.004.
- [5] No. FHWA NHI-05-039. (2005). Micropile design and construction—Reference manual, FHWA NHI-05-039. Department of Transportation. Federal Highway Administration, U. S. Department of Transportation, Washington, United States.
- [6] Bui, D. Van, Nguyen, M. Van, Nguyen, T. D., & Vu, T. N. (2022). A numerically investigate of the improvement of load carrying capacity of square footings utilizing micropiles. Journal of Mining and Earth Sciences, 63(5), 106–117. doi:10.46326/jmes.2022.63(5).10.
- [7] Aboutabikh, M., Soliman, A. M., & El Naggar, M. H. (2020). Performance of hollow bar micropiles using green grout incorporating treated oil sand waste. Journal of Building Engineering, 27, 100964. doi:10.1016/j.jobe.2019.100964.
- [8] Shong, I. L. S., & Chung, F. C. (2003). Design & construction of micropiles. Geotechnical Course for Pile Foundation Design and Construction, 29-30 September 2003, Ipoh, Malaysia.
- [9] Intergovernmental Panel on Climate Change (IPCC). (2014). Mitigation of climate change. Contribution of working group III to the fifth assessment report of the intergovernmental panel on climate change, Cambridge University Press, New York, United States.
- [10] Qian, C. (2022). Application of low-carbon design concept of network energy consumption based on SDN architecture in high-rise residential building design. Alexandria Engineering Journal, 61(4), 3303–3312. doi:10.1016/j.aej.2021.08.063.
- [11] Shen, W., Cao, L., Li, Q., Zhang, W., Wang, G., & Li, C. (2015). Quantifying CO₂ emissions from China's cement industry. Renewable and Sustainable Energy Reviews, 50, 1004–1012. doi:10.1016/j.rser.2015.05.031.
- [12] Madlool, N. A., Saidur, R., Hossain, M. S., & Rahim, N. A. (2011). A critical review on energy use and savings in the cement industries. Renewable and Sustainable Energy Reviews, 15(4), 2042–2060. doi:10.1016/j.rser.2011.01.005.
- [13] Dano, C., Hicher, P.-Y., & Tailliez, S. (2004). Engineering Properties of Grouted Sands. Journal of Geotechnical and Geoenvironmental Engineering, 130(3), 328–338. doi:10.1061/(asce)1090-0241(2004)130:3(328).
- [14] Nouranbakhsh, M., Barkhordari, K., & Ghasemi, S. (2024). Improvement of Sand Soil with Bio-micropiles and Bio-grout Injection in Reinforced Soils. International Journal of Engineering, 37(6), 1076–1084. doi:10.5829/ije.2024.37.06c.04.
- [15] Rentier, E. S., & Cammeraat, L. H. (2022). The environmental impacts of river sand mining. Science of the Total Environment, 838(1), 155877. doi:10.1016/j.scitotenv.2022.155877.
- [16] Walenna, M. A. (2023). Investigating the Consolidation Behaviour of Cement-Bentonite Barrier Materials Containing PFA and GGBS. Civil Engineering Journal, 9(3), 512-530. doi:10.28991/CEJ-2023-09-03-02.
- [17] Avci, E. (2019). Silica Fume Effect on Engineering Properties of Superfine Cement–Grouted Sands. Journal of Materials in Civil Engineering, 31(11), 4019269. doi:10.1061/(asce)mt.1943-5533.0002928.

- [18] Bakar, A. A., & Hashim, M. S. (2023). The grout performance with coal bottom ash as partial sand replacement. *International Conference on Materials Engineering and Manufacturing Systems: Icmems2022*, 2747, 040014. doi:10.1063/5.0113779.
- [19] Çelik, F., Çınar, M., & Akcuru, O. (2022). Utilization of waste bottom ash as mineral additive with partial replacement of cement in geotechnical grouting works based on mechanical features. *Arabian Journal of Geosciences*, 15(14). doi:10.1007/s12517-022-10560-1.
- [20] Lin, C., Wang, M., Liu, X., Li, Z., Zhang, J., & Gao, Y. (2023). Working performance of red mud-based grouting materials mixed with ultrafine limestone and quartz. *Construction and Building Materials*, 383, 131326. doi:10.1016/j.conbuildmat.2023.131326.
- [21] Obebe, M. D., Ikumapayi, C. M., & Alaneme, K. K. (2023). Structural performance evaluation of concrete mixes containing recycled concrete aggregate and calcined termite mound for low-cost housing. *Alexandria Engineering Journal*, 72, 237–246. doi:10.1016/j.aej.2023.03.095.
- [22] Tang, P., Javadi, A. A., & Vinai, R. (2024). Sustainable utilisation of calcium-rich industrial wastes in soil stabilisation: Potential use of calcium carbide residue. *Journal of Environmental Management*, 357, 120800. doi:10.1016/j.jenvman.2024.120800.
- [23] Pastor, J. L., Ortega, J. M., Flor, M., López, M. P., Sánchez, I., & Climent, M. A. (2016). Microstructure and durability of fly ash cement grouts for micropiles. *Construction and Building Materials*, 117, 47–57. doi:10.1016/j.conbuildmat.2016.04.154.
- [24] Danielsen, S. W., Wigum, B. J., Petersen, B., & Hotvedt, O. (2009). Production and Utilisation of Manufactured Sand. State-of-the-art-report. COIN Project report 12, SINTEF Building and Infrastructure, Oslo, Norway.
- [25] Mundra, S., Sindhi, P. R., Chandwani, V., Nagar, R., & Agrawal, V. (2016). Crushed rock sand – An economical and ecological alternative to natural sand to optimize concrete mix. *Perspectives in Science*, 8, 345–347. doi:10.1016/j.pisc.2016.04.070.
- [26] Arulmoly, B., & Konthesingha, C. (2022). Pertinence of alternative fine aggregates for concrete and mortar: a brief review on river sand substitutions. *Australian Journal of Civil Engineering*, 20(2), 272–307. doi:10.1080/14488353.2021.1971596.
- [27] Joel, M. (2010). Use of crushed granite fine as replacement to river sand in concrete production. *Leonardo Electronic Journal of Practices and Technologies*, 9(17), 85–96.
- [28] Li, H., Huang, F., Cheng, G., Xie, Y., Tan, Y., Li, L., & Yi, Z. (2016). Effect of granite dust on mechanical and some durability properties of manufactured sand concrete. *Construction and Building Materials*, 109, 41–46. doi:10.1016/j.conbuildmat.2016.01.034.
- [29] Bacarji, E., Toledo Filho, R. D., Koenders, E. A. B., Figueiredo, E. P., & Lopes, J. L. M. P. (2013). Sustainability perspective of marble and granite residues as concrete fillers. *Construction and Building Materials*, 45, 1–10. doi:10.1016/j.conbuildmat.2013.03.032.
- [30] Zhao, S., Ding, X., Zhao, M., Li, C., & Pei, S. (2017). Experimental study on tensile strength development of concrete with manufactured sand. *Construction and Building Materials*, 138, 247–253. doi:10.1016/j.conbuildmat.2017.01.093.
- [31] TCVN 9205. (2012). Crushed sand for concrete and mortar. National Standard, Hanoi City, Vietnam. (In Vietnamese).
- [32] Ollivier, J. P., Maso, J. C., & Bourdette, B. (1995). Interfacial transition zone in concrete. *Advanced Cement Based Materials*, 2(1), 30–38. doi:10.1016/1065-7355(95)90037-3.
- [33] Bruce, D. A., & Juran, I. (1997). Drilled and Grouted Micropiles: State-of-Practice Review, Volume IV: Case Histories. Department of Transportation, Federal Highway Administration, Washington, United States.
- [34] ASTM C230/C230M-20. (2021). Standard Specification for Flow Table for Use in Tests of Hydraulic Cement. ASTM International, Pennsylvania, United States. doi:10.1520/C0230_C0230M-20.
- [35] ASTM C939-10. (2016). Standard Test Method for Flow of Grout for Preplaced-Aggregate Concrete (Flow Cone Method). ASTM International, Pennsylvania, United States. doi:10.1520/C0939-10.
- [36] UN-EN 14199. (2015). Execution of special geotechnical works – Micropiles. Asociación Española de Normalización, UNE, Madrid, Spain. (In Spanish).
- [37] Chattopadhyaya, B. C., & Saha, S. (1982). Effect of grain size of cohesionless soil on its shear strength characteristics. *Geomech 81: Symposium on Engineering Behaviour of Coarse Grained Soils, Boulders & Rocks*, 21-23 December 1981, Hyderabad, India.
- [38] Li, S., Sha, F., Liu, R., Zhang, Q., & Li, Z. (2017). Investigation on fundamental properties of microfine cement and cement-slag grouts. *Construction and Building Materials*, 153, 965–974. doi:10.1016/j.conbuildmat.2017.05.188.
- [39] Lim, S. K., Tan, C. S., Chen, K. P., Lee, M. L., & Lee, W. P. (2013). Effect of different sand grading on strength properties of cement grout. *Construction and Building Materials*, 38, 348–355. doi:10.1016/j.conbuildmat.2012.08.030.
- [40] Pantazopoulos, I. A., Markou, I. N., Christodoulou, D. N., Droudakis, A. I., Atmatzidis, D. K., Antiohos, S. K., & Chaniotakis, E. (2012). Development of microfine cement grouts by pulverizing ordinary cements. *Cement and Concrete Composites*, 34(5), 593–603. doi:10.1016/j.cemconcomp.2012.01.009.

- [41] Farran, J. (1957). Mineralogical contribution to the study of adhesion between the hydrated constituents of cements and coated materials, Ph.D. Thesis, Toulouse, France. (In French)
- [42] Zimbelmann, R. (1985). A contribution to the problem of cement-aggregate bond. *Cement and Concrete Research*, 15(5), 801–808. doi:10.1016/0008-8846(85)90146-2.
- [43] Jambor, J. (1986). Pore structure and strengths of hardened cement pastes. Proceedings of 8th ICCR, 22-27 September, 1986, Rio de Janeiro, Brazil.
- [44] Akçaoğlu, T., Tokyay, M., & Çelik, T. (2004). Effect of coarse aggregate size and matrix quality on ITZ and failure behavior of concrete under uniaxial compression. *Cement and Concrete Composites*, 26(6), 633–638. doi:10.1016/S0958-9465(03)00092-1.
- [45] Lyu, K., She, W., Chang, H., & Gu, Y. (2020). Effect of fine aggregate size on the overlapping of interfacial transition zone (ITZ) in mortars. *Construction and Building Materials*, 248, 118559. doi:10.1016/j.conbuildmat.2020.118559.
- [46] Elsharief, A., Cohen, M. D., & Olek, J. (2003). Influence of aggregate size, water cement ratio and age on the microstructure of the interfacial transition zone. *Cement and Concrete Research*, 33(11), 1837–1849. doi:10.1016/S0008-8846(03)00205-9.
- [47] Scrivener, K. L., Crumbie, A. K., & Laugesen, P. (2004). The interfacial transition zone (ITZ) between cement pastes and aggregate in concrete. *Interface Science*, 12(4), 411–421. doi:10.1023/B:INTS.0000042339.92990.4c.
- [48] Kang, S. H., Ahn, T. H., & Kim, D. J. (2012). Effect of grain size on the mechanical properties and crack formation of HPRCC containing deformed steel fibers. *Cement and Concrete Research*, 42(5), 710–720. doi:10.1016/j.cemconres.2012.02.011.
- [49] Grandet, J., & Ollivier, J. P. (1980). Study of the formation of hydrated calcium MonoCarb aluminate in contact with a limestone aggregate in a Portland cement paste. *Cement and Concrete Research*, 10(6), 759–770. doi:10.1016/0008-8846(80)90004-6.
- [50] Garboczi, E. J. (1990). Permeability, diffusivity, and microstructural parameters: A critical review. *Cement and Concrete Research*, 20(4), 591–601. doi:10.1016/0008-8846(90)90101-3.
- [51] Monteiro, P. (2006). *Concrete: microstructure, properties, and materials*. McGraw-Hill Publishing, New York, United States.
- [52] Wong, H. S., & Buenfeld, N. R. (2006). Patch microstructure in cement-based materials: Fact or artefact? *Cement and Concrete Research*, 36(5), 990–997. doi:10.1016/j.cemconres.2006.02.008.
- [53] Yuan, C. Z., & Odler, I. (1987). The interfacial zone between marble and tricalcium silicate paste. *Cement and Concrete Research*, 17(5), 784–792. doi:10.1016/0008-8846(87)90041-X.